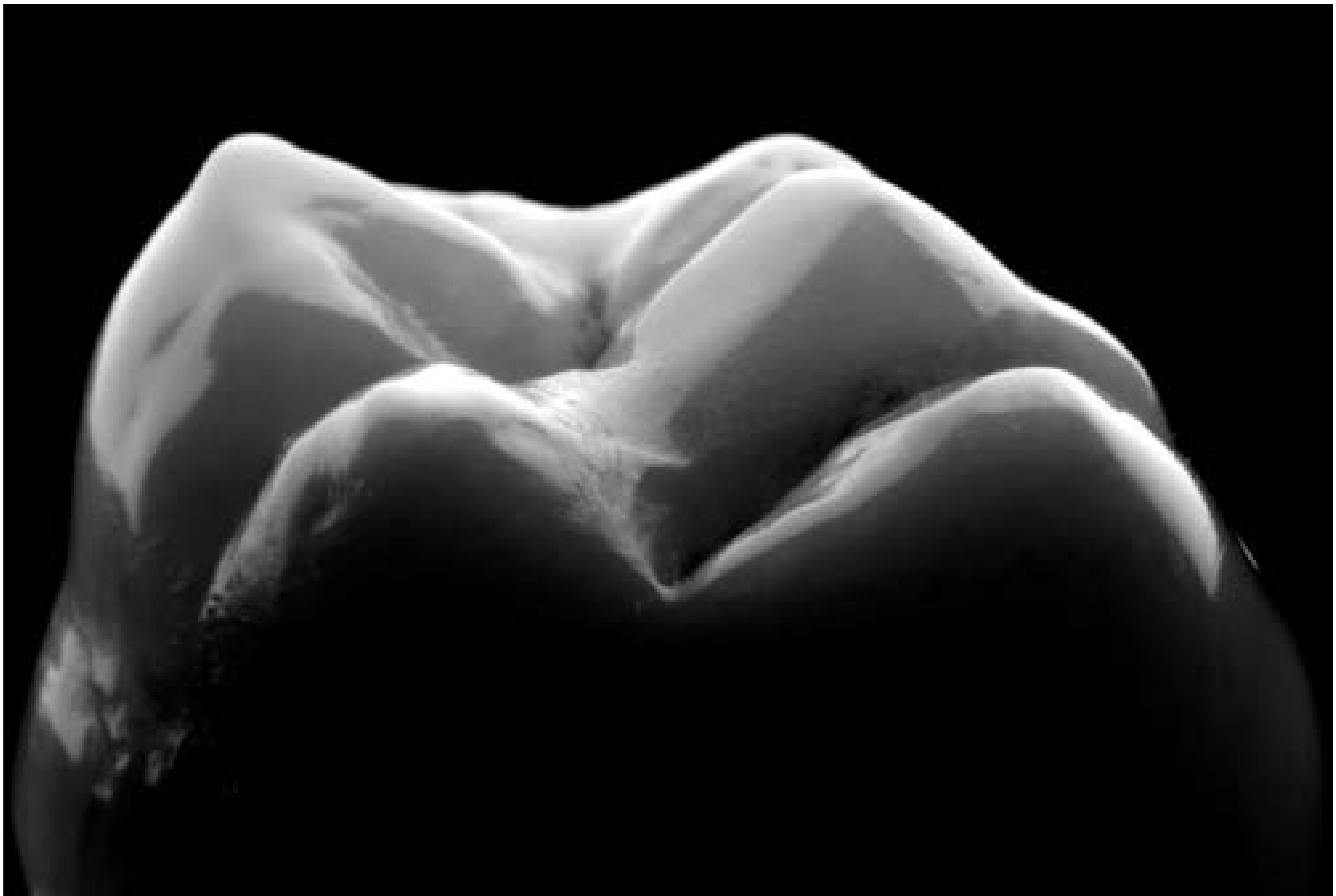

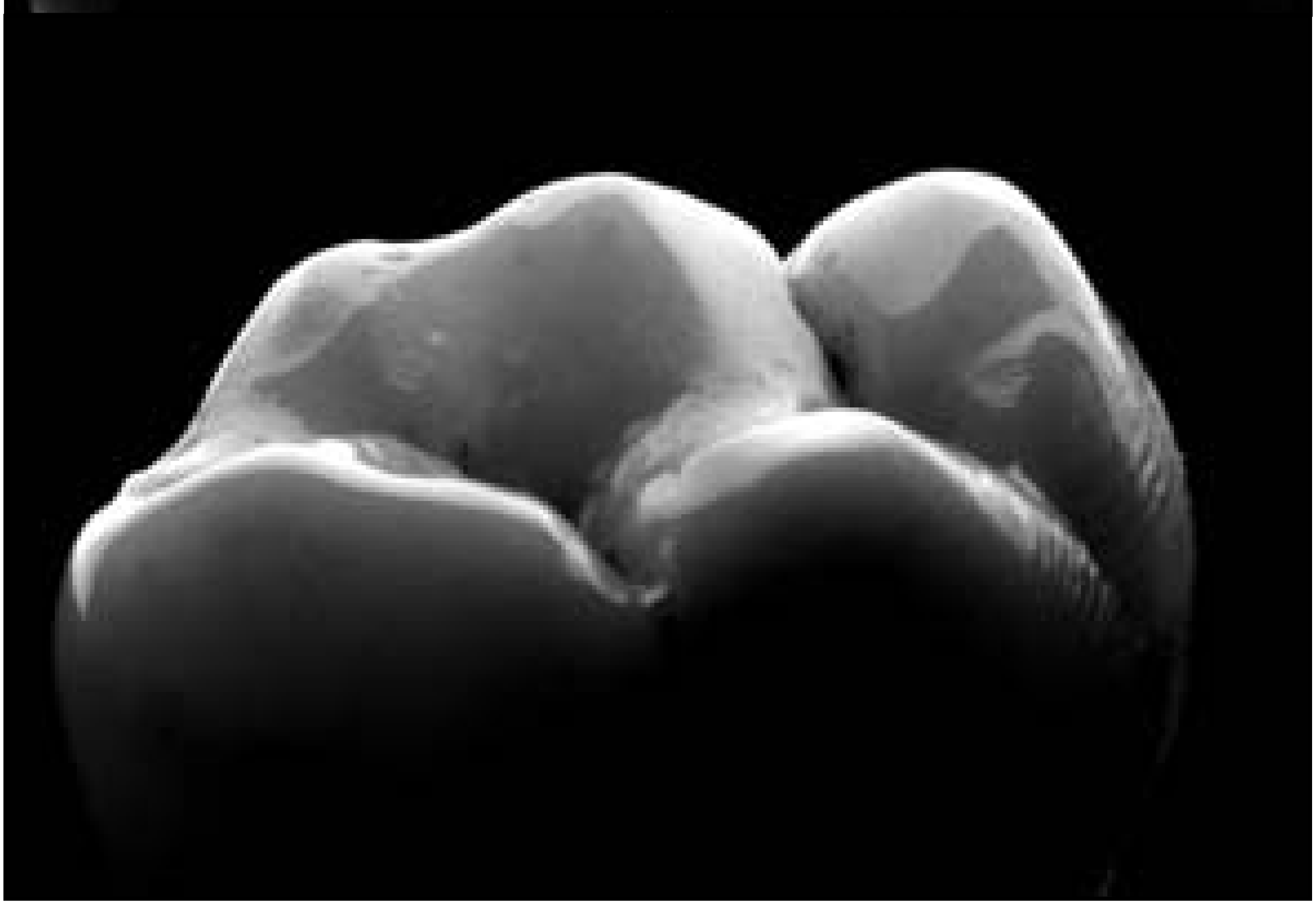

Rationalization of Shape and Related Stress Distribution in Posterior Teeth: A Finite Element Study Using Nonlinear Contact Analysis

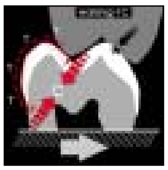

Pascal Magne, Dr Med Dent/Urs C. Belser, Prof Dr Med Dent***

This study considered the loading configuration of intact teeth by using finite element analyses to rationalize the clinical and biologic advantage inherent to posterior tooth shape. The biomechanical behavior of opposing molars was investigated in consideration of different loadcases simulating working, nonworking, and vertical closing micromotions starting in a position close to maximum intercuspation. The resulting stress distribution was assessed in a numerical model, reproducing 2-D buccolingual cross sections of maxillary and mandibular molars. In each case (working/nonworking/closure), the stroke was applied to the mandibular tooth in a stepping procedure (nonlinear contact analysis) until a total external force of 200 N was attained on the contact nodes. The principal stress distribution and modified Von Mises stresses were extracted from the postprocessing files. Vertical loading of the teeth did not generate harmful concentrations of stress. More challenging situations were encountered during working and nonworking micromotions, both of which generated inverted stress patterns. Supporting cusps were generally well protected during both working and nonworking cases (mostly subjected to compressive stresses). Nonsupporting cusps tended to exhibit more tensile stresses. High stress levels were found in the central groove of the maxillary molar during nonworking micromotion and at the lingual surface of enamel of the mandibular tooth during single-contact working micromotion. The occlusal load configuration as well as geometry and hard tissue arrangement had a marked influence on the stress distribution within opposing molars. Additional computations demonstrated the essential role of enamel bridges and crests to protect the crown from harmful tensile stresses. (Int J Periodontics Restorative Dent 2002;22:xxx–xxx.)

*Senior Lecturer, Department of Prosthodontics, School of Dental Medicine, University of Geneva, Switzerland; and Adjunct Associate Professor, Department of Oral Science, University of Minnesota, Minneapolis.

**Professor and Chair, Department of Prosthodontics, School of Dental Medicine, University of Geneva, Switzerland,

Reprint requests: Dr Pascal Magne, University of Geneva, School of Dental Medicine, Department of Prosthodontics, 19 rue Barthélemy-Menn, CH-1205 Genève, Switzerland. e-mail: Pascal.Magne@medecine.unige.ch

Reproducing the original performance of the intact tooth (“biomimetics”) should be a driving force in restorative dentistry.[1] It requires fundamental understanding of the natural tooth with regard to its intimate structure, biology, morphology, and external shape (Fig 1). For posterior teeth, chief advances have resulted from the study and understanding of cuspal flexure and plastic yielding, which represent key parameters in the performance of the tooth-restorative complex.[2,3] Subclinical cuspal microdeformation, ie, below the threshold of chairside observation, was identified in the early 1980s,[2,4,5] and it is now well accepted that intact teeth demonstrate cuspal flexure because of their morphology and occlusion. Restorative procedures can increase cuspal movement under occlusal load,[2,6] which may result in altered strength, fatigue fracture, and cracked tooth syndromes.[7–9] Such knowledge allowed the development of methods to improve fracture resistance of teeth[10,11] through various forms of complete or partial coverage[12–14] and by introducing

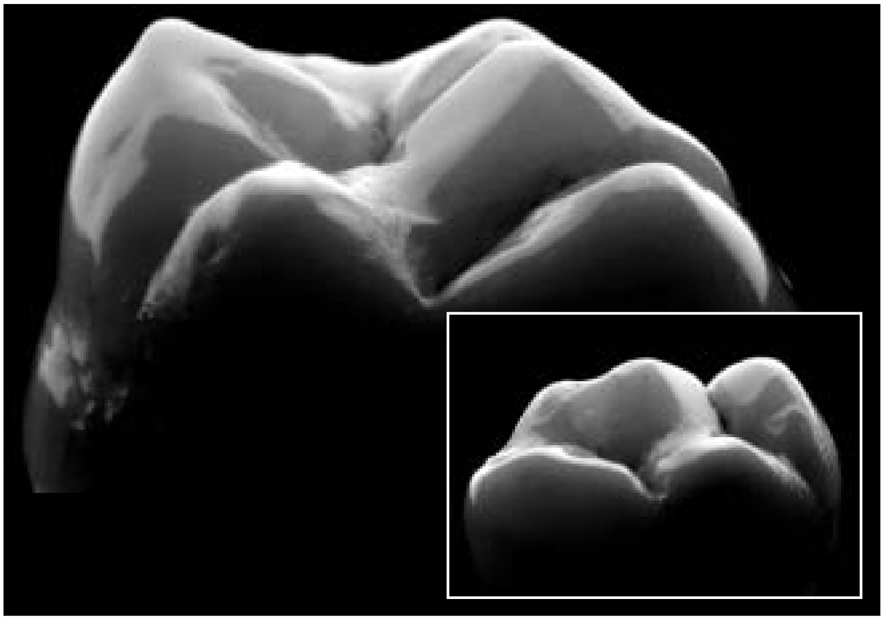

Fig 1 *Intact maxillary molar, occlusal views from distal* (top) *and buccal angles* (bottom). *The masticatory surface is characterized by the succession of enamel crests and deep grooves.*

the more conservative adhesive techniques.[3,15,16]

Most of the in vitro investigations mentioned above were carried out using nondestructive strain gauge methods along with load-to-failure tests. These traditional "load-point" experiments provide insights into a number of biomechanical issues, yet they do not reveal the stress distribution within the tooth-restoration complex during biting and clenching. Knowledge of stress distribution is of paramount importance in the biomimetic approach (especially in the optimization of adhesive restorative techniques), but requires complex modeling tools such as the finite element (FE) method. In FE analysis, a large structure is divided into a number of small simple-shaped elements, for which individual deformation (strain and stress) can be more easily calculated than for the entire undivided structure. By solving the deformation of all the small elements simultaneously, the deformation of the structure as a whole can be assessed. Using the traditional biophysical knowledge database in a rational validation process, FE analysis has been significantly refined during recent years.[17] Nowadays, experimental-numerical approaches undoubtedly represent the most comprehensive in vitro investigation methods. The present work used two-dimensional FE models, the accuracy of which, considered in a buccolingual cross section, has been demonstrated and validated on several occasions by experimental strain measurements on both anterior and posterior teeth.[1,4,5,18]

The aim of this study was to describe the biomechanical response of intact opposing molars in terms of stress and strain distribution based on 2-D FE simulations. Current literature provides little information about the effect of realistic biting configurations on the biomechanical behavior of posterior teeth. Special attention was therefore given to the simulation of opposing contacts during micromotions including clenching, working, and nonworking excursions.

Method and materials

Mesh generation and material properties (preprocessing)

Buccolingual cross sections of natural maxillary and mandibular molars were digitized using a charge coupled device camera (Sony DXC-151A) attached to a stereomicroscope (Olympus SZH10) and an image-analysis software program (Optimas 5.22). The contours of the enamel, dentin, and pulp areas were

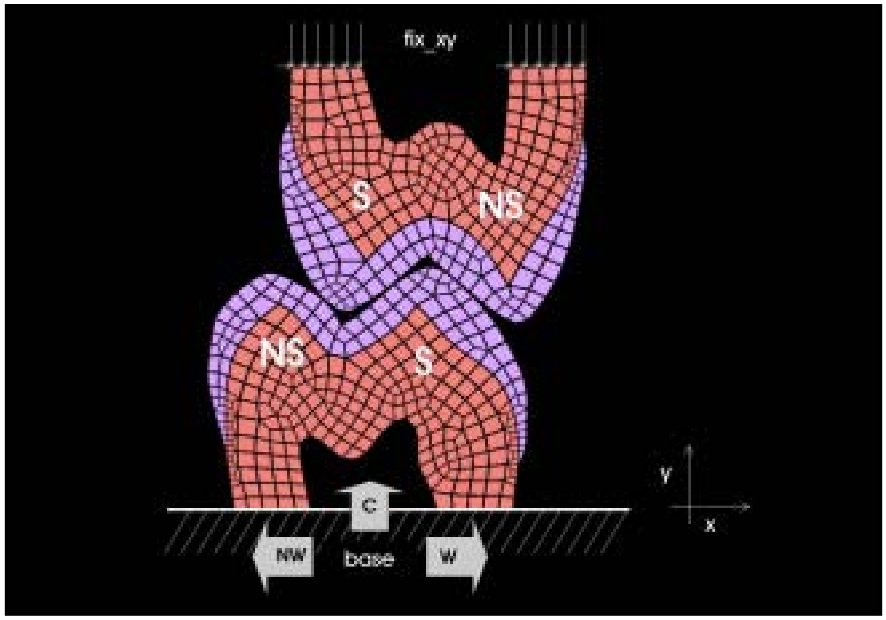

Fig 2 *Two-dimensional FE model of maxillary and mandibular molars consisting of 606 elements and 700 nodes. The cervical part of enamel and its supporting dentin were intentionally designed with a higher concentration of elements for a better representation of the thin enamel. The first row of nodes at the root base of the maxillary molar was fixed in x and y axes* (thin arrows), *and the micromotion was applied to the mandibular molar (*W *= horizontal working motion;* NW *= horizontal nonworking motion;* C *= vertical motion) through the stroke control of a rigid base.* S *= supporting cusps;* NS *= nonsupporting cusps.*

manually traced using a PC workstation and graphic software (Freelance Graphics, Lotus). An image-processing program (NIH Image, developed at the Research Services Branch of the National Institute of Mental Health) was used to record the coordinates of all of the structures and defined contours. These geometric data were then transferred to an interactive FE program for mesh generation and preprocessing (Mentat 2000, MSC Software). Although teeth are 3-D structures, a 2-D FE model with plane-strain elements (linear, four-node, isoparametric, and arbitrary quadrilateral) was chosen (Fig 2). A 3-D model, although more realistic, would have resulted in coarser meshes. The increased memory requirements for 3-D models combined with the nonlinear nature of this analysis would not have allowed fine representation of the geometry. As reported by Versluis et al,[19] a correct ratio of moduli (enamel:dentin) is necessary for a qualitative analysis. Moduli of 50 GPa and 12 GPa were chosen for enamel and dentin, respectively, yielding a ratio of 4.2. Poisson's ratios of 0.23 for dentin[20] and 0.30 for enamel[21] were assumed.

Boundary conditions, loadcase, and data processing

Contours of opposing teeth were positioned as close as possible to maximum intercuspation, but without contacts. Teeth were defined as deformable contact bodies. Fixed zero displacement in both the horizontal and vertical directions was assigned to the cut plane of the root of the maxillary molar, approximately 1.5 mm beyond the cementoenamel junction. The motion was applied to the mandibular tooth through the displacement of a rigid base (nondeformable body) glued to the cut plane of the root. Contact between bodies in Mentat 2000 software was controlled according to the deformable-deformable method ("double-sided," ie, presence of two deformable bodies) in a static mechanical loadcase with a stepping procedure (50 steps). Preliminary testing included the application of Coulomb friction (enamel friction coefficient of 0.4), but this feature was ultimately abandoned because no difference could be detected, probably because of the very limited sliding of the cusps. In a first approach, four different loadcases were simulated:

1. *Working micromotion on two contacts.* The movement of the base simulated a working motion ("W" in Fig 2): three steps of 16 µm were required to reach contact in two locations (Fig 3a). The

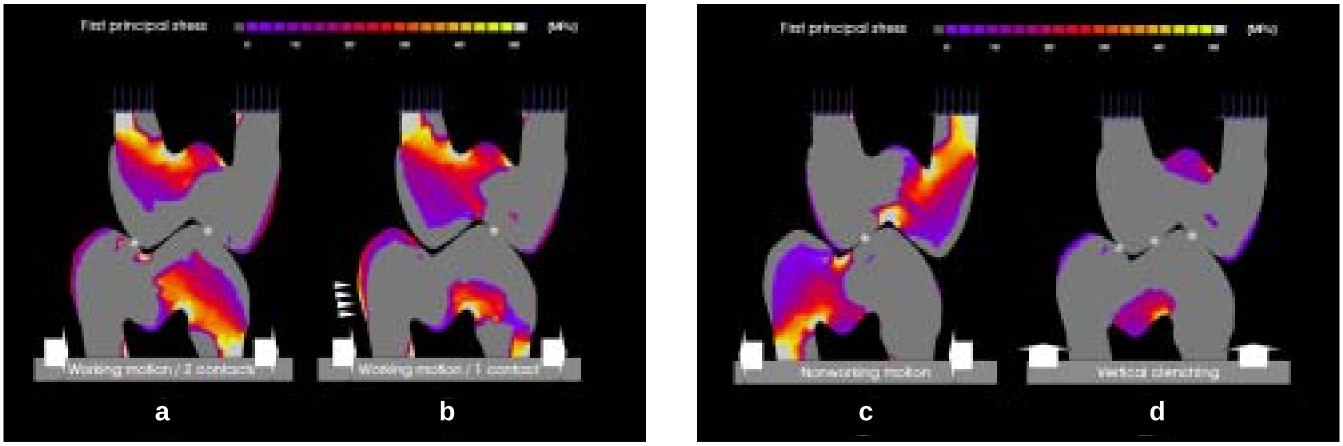

Fig 3 *First principal stresses within the molar cross sections for each loadcase. Negative values of stress appear in gray and delineate the areas of compressive stresses. Color shadings indicate the different levels of tensile stresses. In each loadcase* (a *to* d), *the sum of external forces on the contact nodes is ≈ 200 N. Note the tensile stresses at the lingual surface in Fig 3b* (arrowheads). * = *area of contact nodes*

motion continued for nine additional steps (144 µm) to reach a total force of ≈ 200 N on the contact nodes.

2. *Working micromotion on one contact.* The morphology of the lingual cusp of the mandibular molar was slightly modified to avoid contact during the working motion: three steps of 16 µm were required to reach contact between the buccal cusps only (Fig 3b). The motion continued for 10 additional steps (160 µm) to reach a total force of ≈ 200 N on the contact nodes.
3. *Nonworking micromotion.* The movement of the base simulated a nonworking motion (“NW” in Fig 2): four steps of 16 µm were required to reach contact (Fig 3c). The motion continued for 10 additional steps (160 µm) to reach a total force of ≈ 200 N on the contact nodes.
4. *Vertical micromotion.* The movement of the base simulated a vertical closure (“C” in Fig 2): seven steps of 8 µm were required to reach contact in three locations (Fig 3d). The motion continued for five additional steps (40 µm) to reach a total force of ≈ 200 N on the contact nodes. At all times in this specific case, the mandibular molar was allowed to move laterally on its base (along the x axis), which ultimately provided an optimal centering in maximum intercuspation.

The stress distribution within both molars was solved using the MARC 2000 Analysis solver (MSC Software). The postprocessing file was accessed through Mentat.

Results

In a systematic approach to understand the deformation mode of the tooth, it is appropriate to analyze stresses in a direction for which the x and y components of stresses will display their maximum values. The resulting analysis (Fig 3) outlines the principal stresses in the form of areas of compression and tension.

Working motions

Both loadcases simulating a working motion (Figs 3a and 3b) generated on the supporting cusps compressive stress in the enamel and tension in the major area of dentin. However, a definite portion of enamel at the nonsupporting cusps (buccal surface of the maxillary tooth and lingual surface of the mandibular one), was subjected to tensile stresses, whereas underlying dentin was totally under compression in these cusps. Extremely high lingual tensile forces were generated by the working case with only one contact. On the other hand, high tensile stresses were found at the central sulcus of the mandibular molar in the working case with two contacts. Finally, both working cases generated similar stresses at the pulp ceiling, ie, marked tension at the buccal pulp horn of the mandibular molar and at the palatal pulp horn of the maxillary tooth.

Nonworking motion

The stress pattern generated by the nonworking motion (Fig 3c) was exactly the reverse of that of the working motion cases. The enamel surface at the nonsupporting cusps was subjected to compressive stresses, whereas underlying tooth substance was under tension. Except for slight portions of the enamel surface, most parts of the supporting cusps were subjected to compression. Inversely to the working motion cases, tension was found here at the lingual pulp horn of the mandibular molar and at the buccal pulp horn of the maxillary tooth. This nonworking motion case was also characterized by the elevated tensile stresses at the central groove of both teeth, especially the maxillary molar.

Vertical closure

The vertical closing motion (Fig 3d) generated mainly compressive stresses. Only slight tensile stresses were found at the external surface of nonsupporting cusps and at the pulp ceiling.

Modified Von Mises failure citerion

It is important to mention that both enamel and dentin are brittle materials that present a higher strength in compression than in tension. The strength differential effect, namely the ratio between compressive strength and tensile strength, has been incorporated in a failure criterion for brittle types of materials: the modified Von Mises criterion (mVM).[22] Therefore, Fig 4 illustrates the stress distribution at the surface of the teeth using the mVM. Only a very limited amount of mVM stresses were found during closure. The maxillary molar was characterized by the elevated tensile stresses responsible for the mVM stress peak at the central groove during the nonworking motion. Interestingly, the same nonworking motion generated the most harmful stresses found in the cervical enamel among all loadcases. In the mandibular tooth, the different cases generated similar mVM curves, except for the lingual surface of enamel during the working motion with a single contact, which exhibited higher amounts of mVM stresses.

Discussion

Relevance of selected boundary conditions and loadcases

There are several reasons why micromotions starting from an intercuspal position were chosen for this simulation: *(1)* occlusal contacts close to the intercuspal position are probably involved in some critical stages of food breakdown, *(2)* most tooth contact during mastication seems to occur in this position,[23] and *(3)* maximum masticatory force is exerted by closing muscles in this seemingly motionless state.[24] The extent of micromotion was chosen to reach a bite force of ≈ 200 N, which corresponds to the low range of maximum bite force or bite force during bruxism.[25,26]

The root was not modeled, as it may be assumed that the overall stress distribution in the coronal portion is only marginally affected by the root area under the simulated boundary conditions. Generally speaking, when local stress distributions in a crown are studied, fixation of the model is prescribed along the cross section of the root. With the model being fixed at the cut plane of the root, a stress is generated in this area. Normally, this stress would be diffused throughout the periodontal membrane and, as here, not influence coronal events. Owing to the above-mentioned reasons, no conclusions can be drawn from the high levels of tensile stresses encountered in the root portion of dentin.

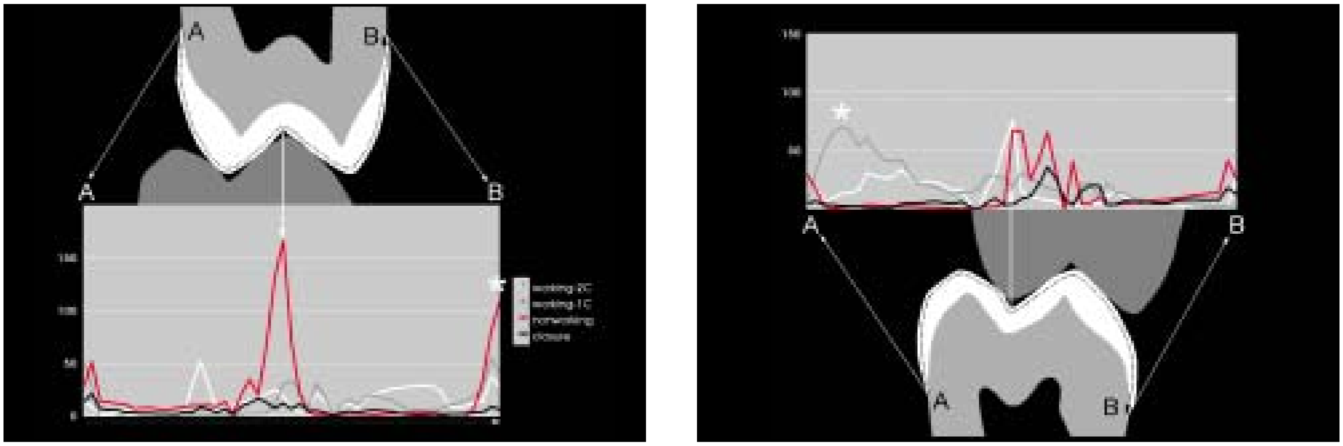

Fig 4 *Modified Von Mises stresses (MPa) for each loadcase. Path plot proceeds along the enamel surface* (dotted arrows) *from the lingual/palatal cementoenamel junction* (A) *to the buccal side* (B). *Note the stress peak at the sulcus of the maxillary tooth during the nonworking motion* (red curve) *and the elevated stresses at the buccal cervical aspect in the same curve* (*, left plot). *Note also the stress peak at the lingual surface of the mandibular molar during the working motion with a single contact* (*, right plot, gray curve).

The biomimetic approach

The results presented here might be questioned because they have been produced in an FE environment. The methods used in this study, however, are based on several preexisting validation studies that have proven the relevance of these concepts.[1,4,5,18] Even though some differences can remain between reality and the FE environment, there are still at least two reasons that justify the use of numerical modeling: *(1)* it is able to reveal the otherwise inaccessible stress distribution within the tooth-restoration complex, and *(2)* it has proven to be an essential tool in the thinking process for the understanding of tooth biomechanics and the biomimetic approach. Biomimetics is a newly emerging interdisciplinary material science[27] involving investigation of both structures and physical functions of biologic "composites" and the designing of new and improved substitutes. In restorative dentistry, it starts with the understanding of hard tissue arrangement and related stress distribution within the intact tooth.[1,28] Chief advances have resulted from such an approach in the field of anterior bonded ceramic restorations.[29] New restorative approaches do not aim to create the strongest restoration, but rather a restoration that is compatible with the mechanical and biologic properties of underlying dental tissues—the biomimetic principle. Enamel, dentin, and modern dental materials (ceramics, composite resins) are characterized by their brittle behavior. It is of paramount importance to locate harmful stresses during function, which constituted one aim of the present study.

General stress patterns

Inversely to anterior teeth, cusps do not deform under load as simple cantilever beams.[30] The deformation mode is complicated by the numerous possibilities in the application of loads (working, nonworking, closure). General assumptions claiming the harmful effect of lateral loading have been confirmed in the present work. Vertical loading of the tooth (in the direction of its main axis) did not generate harmful concentrations of stress. More challenging situations were encountered during working and nonworking micromotions, both of which generated inverted stress patterns. From the current analysis, it appears that supporting cusps are generally well protected during both working and nonworking loadcases (mostly subjected to compressive stresses).

Fig 5 *Deformation mode of the lingual cusp during the single-contact working loadcase. The oblique compression of lingual dentin* (C = compression, large red dashed arrows) *is buckling the lingual cusp and stretching the outer enamel shell.* T = *tension.*

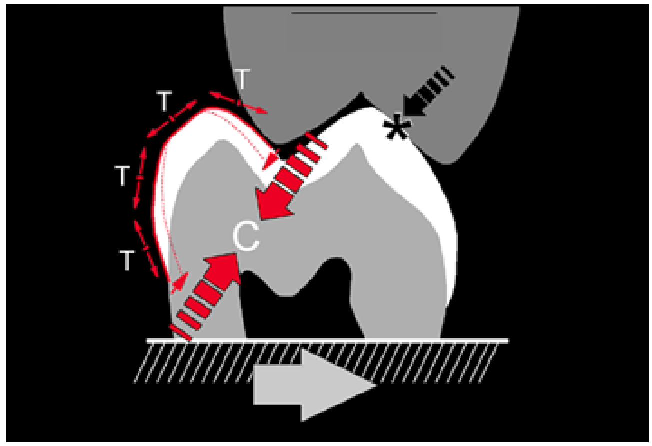

Nonsupporting cusps tend to exhibit more tensile stresses. The most surprising effect was found in the form of a stress peak at the lingual surface of enamel (mandibular molar) in the single-contact working case. It can be explained by the massive oblique compression of dentin in the lingual cusp. The surface of enamel must stretch to conform to the buckling of the cusp (Fig 5). The presence of a second contact between the palatal and lingual cusps significantly reduced that phenomenon by transferring tension in the central groove.

Natural protective mechanisms of the intact tooth

High levels of mVM stresses were found at certain locations in enamel, especially in the central groove (maxillary tooth during nonworking motion in Fig 4). This situation must be evaluated in view of additional data to understand the effect of geometry and shape on the stress distribution. An experimental-numerical study carried out on anterior teeth[31] demonstrated low stress levels in enamel surfaces of maximum convex curvature, namely the cingulum and the cervical part of the facial surface of incisors. It was concluded that convex surfaces with thick enamel raise less concentrated stresses than concave areas, which tend to concentrate stresses. These principles can be applied to posterior teeth. Figure 5 illustrates the variable morphology of the central sulcus within the same tooth, which can exhibit a marked crest or enamel bridge (Fig 6a) or a deep fissure with an extreme concavity (Fig 6b). Additional computations were carried out to explore the effect of these two extreme geometric designs on the mVM stresses. The results are presented in Fig 7: Enamel bridging not only reduces the stresses locally (see the sulcus of the maxillary molar), but can also protect distant enamel (see the lingual enamel of the mandibular tooth). The dentinoenamel junction (DEJ) constitutes another crucial element that must be mentioned among the natural protective mechanisms of the tooth. The crack-arresting effect of dentin and of the thick collagen fibers at the DEJ[32] compensate for the inherently brittle nature of enamel. The complex fusion found at the DEJ can be regarded as a fribril-reinforced bond,[33] and scanning electron microscopic fractographs of DEJ specimen have demonstrated crack deflection to another fracture plane when forced through the DEJ zone.[32]

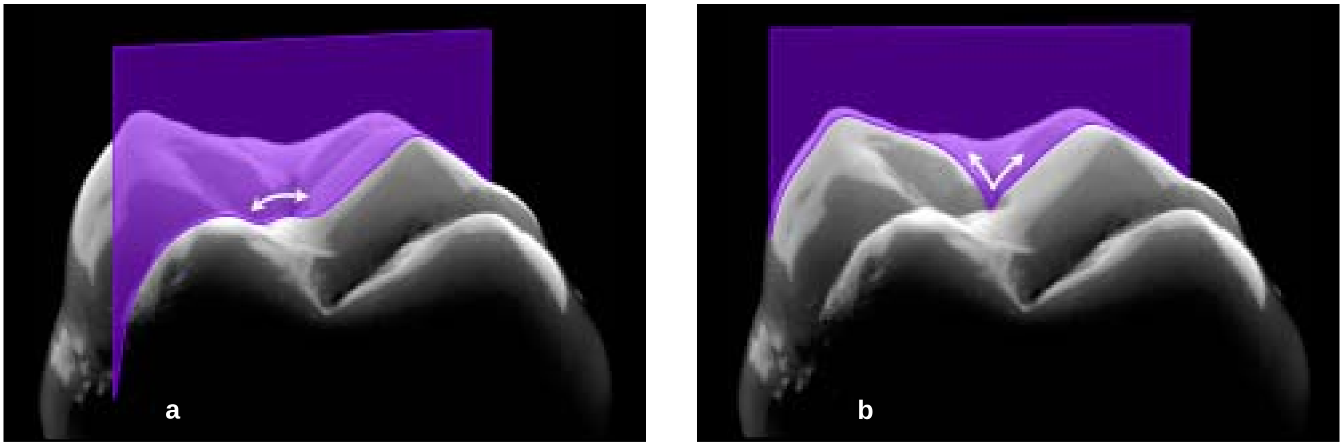

Fig 6 *The same tooth can display extreme morphologic types within the occlusal table, either with an enamel bridge or crest* (a) *or a deep fissure* (b) *according to the cross-sectional area. These elements were considered for additional computations presented in Fig 7.*

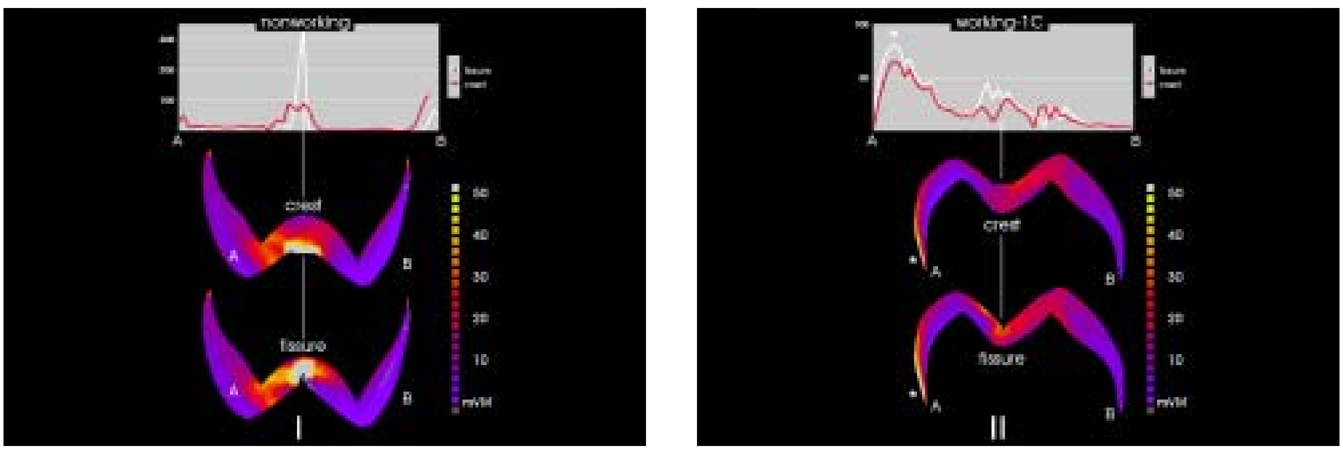

Fig 7 *Modified Von Mises stresses (MPa) for the two additional loadcases with altered central grooves (crest and fissure):* (I) *maxillary molar during nonworking motion, and* (II) *mandibular tooth during working motion with a single contact. Same path plot as in Fig 4* (A *to* B). *Note marked reduction of stress peak at sulcus of maxillary tooth in the presence of the crest* (red curve). *Note also the reduction of stresses at lingual surface of mandibular molar because of the distant presence of the enamel bridge.*

Conclusions

Measurements made on numerical models (nonlinear contact analysis) demonstrated that stress distribution in posterior teeth is determined by the occlusal load configuration (working versus nonworking versus vertical micromotions) as well as geometry and hard tissue arrangement.

- Vertical loading of the tooth (in the direction of its main axis) did not generate harmful concentrations of stress compared to working and nonworking strokes.
- Working and nonworking strokes generated opposite stress patterns.
- Supporting cusps were generally well protected by compressive stresses, whereas nonsupporting cusps tended to exhibit more tensile stresses.

[AU: Please verify ref 11 info. (Ref 10 lists a different author for the same chapter.)]

[AU: Is ref 12 an abstract? If so, please list abstract number.]

- High stress levels were found in the central groove of the maxillary molar during nonworking micromotion and at the lingual surface of enamel of the mandibular tooth during single-contact working micromotion.
- Enamel bridges and crests proved to be essential mechanisms to protect crown biomechanics.

Acknowledgments

This study was supported in part by the Minnesota Dental Research Center for Biomaterials and Biomechanics (image processing and numerical modeling) and the Swiss Foundation for Medical-Biological Grants. The authors wish to express their gratitude to Dr Antheunis Versluis for his help in refining the finite element modeling and numerical output.

References

1. Magne P, Douglas WH. Rationalization of esthetic restorative dentistry based on biomimetics. J Esthet Dent 1999;11:5–15.
2. Douglas WH. Considerations for modeling. Dent Mater 1996;12:203–207.
3. Morin D, Delong R, Douglas WH. Cusp reinforcement by the acid-etch technique. J Dent Res 1984;63:1075–1078.
4. Morin DL, Douglas WH, Cross M, Delong R. Biophysical stress analysis of restored teeth: Experimental strain measurements. Dent Mater 1988;4:41–48.
5. Morin DL, Cross M, Voller VR, Douglas WH, Delong R. Biophysical stress analysis of restored teeth: Modeling and analysis. Dent Mater 1988;4:77–84.
6. Assif D, Marshak BL, Pilo R. Cuspal flexure associated with amalgam restorations. J Prosthet Dent 1990;63:258–262.
7. Cameron CE. The cracked tooth syndrome. J Am Dent Assoc 1964;68: 405–411.
8. Cameron CE. The cracked tooth syndrome: Additional findings. J Am Dent Asssoc 1976;93:971–975.
9. Cavel WT, Kelsey WP, Blankenau RJ. An in vivo study of cuspal fracture. J Prosthet Dent 1985;53:38–42.
10. Hood JAA. Methods to improve fracture resistance of teeth. In: Vanherle G, Smith DC (eds). International Symposium on Posterior Composite Resin Restorative Materials. St Paul, Minn, 1985:443–450. **[AU: Who is the publisher?]**
11. Douglas WH. Methods to improve fracture resistance of teeth. In: Vanherle G, Smith DC, eds. International Symposium on posterior composite resin restorative materials. St Paul, Minn, 1985:433–441.
12. Malcolm PJ, Hood JAA. The effect of cast restorations in reducing cusp flexibility in restored teeth. J Dent Res 1971;56:D207.
13. Reeh ES, Douglas WH, Messer HH. Stiffness of endodontically-treated teeth related to restoration technique. J Dent Res 1989;68:1540–1544.
14. Linn J, Messer HH. Effect of restorative procedures on the strength of endodontically treated molars. J Endod 1994;20: 479–485.
15. McCullock AJ, Smith BG. In vitro studies of cusp reinforcement with adhesive restorative material. Br Dent J 1986;161: 450–452.
16. Macpherson LC, Smith BG. Reinforcement of weakened cusps by adhesive restorative materials: An in-vitro study. Br Dent J 1995;178:341–344.
17. Korioth TWP, Versluis A. Modeling the mechanical behavior of the jaws and their related structures by finite element (FE) analysis. Crit Rev Oral Biol Med 1997;8:90–104.
18. Magne P, Douglas WH. Porcelain veneers: Dentin bonding optimization and biomimetic recovery of the crown. Int J Prosthodont 1999;12:111–121.
19. Versluis A, Douglas WH, Cross M, Sakaguchi RL. Does an incremental filling technique reduce polymerization shrinkage ? J Dent Res 1996;75:871–878.
20. Watts DC, Mowafy OM, Grant AA. Temperature-dependence of compressive properties of human dentin. J Dent Res 1987;66:29–32.
21. Craig RG. Restorative Dental Materials, ed 6. St Louis: Mosby, 1980:76.
22. De Groot R, Peters MCRB, De Haan YM, Dop GJ, Plasschaert AJM. Failure stress criteria for composite resin. J Dent Res 1987;66:1748–1752.
23. Pameijer JH, Glickman I, Roeber FW. Intraoral occlusal telemetry. 3. Tooth contacts in chewing, swallowing and bruxism. J Periodontol 1969;40:253–258.
24. Gibbs CH. Electromyographic activity during the motionless period in chewing. J Prosthet Dent 1975;34:35–40.
25. Miura H, Watanabe S, Isogai E, Miura K. Comparison of maximum bite force and dentate status between healthy and frail elderly persons. J Oral Rehabil 2001;28: 592–595.
26. Nishigawa K, Bando E, Nakano M. Quantitative study of bite force during sleep associated bruxism. J Oral Rehabil 2001; 28:485–491.
27. Sarikaya M. An introduction to biomimetics: A structural viewpoint. Microsc Res Technol 1994;27:360–375.
28. Magne P, Douglas WH. Rationalization of esthetic restorative dentistry based on biomimetics. J Esthet Dent 1999;11:5–15.
29. Magne P, Perroud R, Hodges JS, Belser U. Clinical performance of novel-design porcelain veneers for the recovery of coronal volume and length. Int J Periodontics Restorative Dent 2000;20:441–457.
30. Jantarat J, Panitvisai P, Palamara JE, Messer HH. Comparison of methods for measuring cuspal deformation in teeth. J Dent 2001;29:75–82.
31. Magne P, Versluis A, Douglas WH. Rationalization of incisor shape: Experimental-numerical analysis. J Prosthet Dent 1999; 81:345–355.
32. Lin CP, Douglas WH. Structure-property relations and crack resistance at the bovine dentin-enamel junction. J Dent Res 1994;73:1072–1078.
33. Lin CP, Douglas WH, Erlandsen SL. Scanning electron microscopy of type I collagen at the dentin-enamel junction of human teeth. J Histochem Cytochem 1993; 41:381–388.